Colloids and Surfaces B: Biointerfaces 136 (2015) 314–322



Colloids and Surfaces B: Biointerfaces

journal homepage: www.elsevier.com/locate/colsurfb

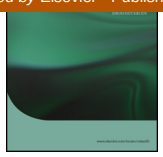

# Nitroxide malonate methanofullerene as biomimetic model of interaction of nitroxide species with antioxidants

N.B. Melnikova[a,*], V.M. Korobko[b], M.V. Gulenova[b], V.P. Gubskaya[c], G.M. Fazlleeva[c], O.E. Zhiltsova[a], E.N. Kochetkov[a], A.I. Poddel'sky[b,d], I.A. Nuretdinov[c]

[a] Department of Pharmaceutical Chemistry, Nizhny Novgorod State Medical Academy, Minin sq., 10/1, 603600 Nizhny Novgorod, Russian Federation
[b] Lobachevsky State University of Nizhni Novgorod, 23 Gagarin Avenue, 603950 GSP-43, Russian Federation
[c] A.E. Arbusov Institute of Organic and Physical Chemistry, Kazan Scientific Center, Russian Academy of Sciences, Arbuzov str. 8, 420088 Kazan, Russian Federation
[d] G.A Razuvaev Institute of Organometallic Chemistry, Russian Academy of Sciences, 49 Tropinina str., 603137 GSP-445, Russian Federation

ARTICLE INFO

*Article history:*
Received 21 May 2015
Received in revised form 12 August 2015
Accepted 14 September 2015
Available online 18 September 2015

*Keywords:*
Biomimetic model of nitroxide species
Nitroxide malonate methanofullerene
Antioxidant
Cytochrome c
Monolayers

ABSTRACT

Bis-nitroxide malonate methanofullerene $(NO^{\bullet})_2$-MF was studied as a biomimetic model of reduction–oxidation activity with natural compounds—cytochrome *c* (cyt *c*), dihydroquercetin (DHQ), ascorbic acid (AA) and synthetic drug—1-(β-oxyethyl)-4,6-dimethyl-1,2-dihydro-2-oxopyrimidine (xymedon®).

$(NO^{\bullet})_2$-MF may be used as the component of Langmuir monolayers on an aqueous subphase and as the adsorbate on silica gel. The activity of $(NO^{\bullet})_2$-MF in the reaction with cyt *c* was compared with the effect of nitroxide species such as gaseous nitric oxide, 2,2,6,6-tetramethylpiperidine-1-oxyl radical (TEMPO) by using UV–vis and EPR-spectra. It has been shown, that iron(III) in cyt $c^{3+}$ under action $(NO^{\bullet})_2$-MF was reduced up to iron(II), similar effect was observed under the influence of gaseous NO in aqueous solution, but reduction of iron(III) in heme cyt *c* was reversible in the presence of TEMPO. Therefore, the state of Fe-heme in cyt *c* can be used as the indicator of the interaction of cyt *c* with nitroxide species *in vitro*.

The interaction of cyt *c*, DHQ, xymedon® with $(NO^{\bullet})_2$-MF monolayers was confirmed by the increasing of limiting area $A_0$ from 0.88 $nm^2$ up to 1.70 $nm^2$ of $(NO^{\bullet})_2$-MF on the aqueous subphase, by the paramagnetism and UV–vis spectral data changes. These results can be explained by appearance of oxoammonium ion $(NO^{+})_2$-MF adlayers and monolayers.

The antioxidant and regenerating effects were shown when treating wounds by xymedon® in the presence of additives (0.001%) of $(NO^{\bullet})_2$-MF in the experiments on the rats.



## 1. Introduction

At present, nitric oxide (NO) is regarded to be one of the most important process control agents *in vivo*, such as endothelial relaxation called "endothelium-derived relaxing factor (EDRF)", nerve signal transmission being the second messenger in the cellular signaling pathways, gene transcription and translation [1]. Biological synthesis of NO is connected to cardiovascular and immune systems and ensures antibacterial, cytotoxic, anti-inflammatory and antioxidant actions *in vivo* [2,3]. It was proved that biotransformation of NO and its related N-oxides occurs via different metabolic routes within the body. The major oxidative metabolites are presented nitrite and nitrate (Supporting information Eqs. (1)–(3)) [4]. On the other hand, NO has been implicated in a variety of different diseases [5]. The reaction NO with either oxygen or superoxide anion proves its toxicity and it leads to direct genotoxicity mediated by $N_2O_3$ and peroxynitrite (Supporting information Eqs. (4) and (5)) or to indirect genotoxicity. Such ambiguous behavior (antioxidant and oxidant effects) is typical for superoxide dismutase (SOD) that takes part in consequent oxidation and reduction reactions under the influence of peroxide radicals, giving superoxide anion.

Nitroxide radicals refer to a unique group of synthetic compounds being antioxidants [6]. Stable cyclic nitroxides such as TEMPO (2,2,6,6-tetramethylpiperidine-1-oxyl radical) having an effective antioxidant properties and they can be used as superoxide dismutase (SOD) mimics. Initially, TEMPO is disproportionated into TEMPOH and the *N*-oxo-ammonium ion (Supporting information

* Corresponding author.
*E-mail addresses:* melnikovanb@gmail.com, chem-pharm@yandex.ru (N.B. Melnikova).

http://dx.doi.org/10.1016/j.colsurfb.2015.09.026

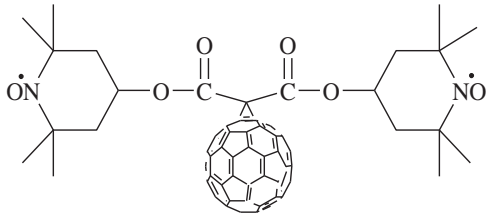

**Scheme 1.** Bis-$(NO^{\bullet})_2$-methanofullerene $(NO^{\bullet})_2$-MF.

Eq. (1)). Then, the *N*-oxo-ammonium ion can act as a well-known oxidant [7].

The antioxidative activity of nitroxides is attributable to several reaction pathways and primarily to the catalytical removal of superoxide through reactions (Supporting information Eqs. (2) and (3)), and to reduction–oxidation of redox-active transition metals through reactions (Supporting information Eq. (4)) [8,9].

The interactions of nitric oxide and iron are the most important biological reactions involving NO. Unlike carbon monoxide or oxygen, NO can also bind reversibly to ferric ion. NO interacts with heme proteins, for e.g. with cytochrome *c* (cyt c), forming nitrosyl complexes [10–12]. Nitrosyl complexes can modify the peroxidase activity of cyt c and control the apoptosis, correspondingly. It was shown, that nitroxides influence catalase-like activity relating to heme proteins, too [9] and to SOD inhibitable cyt *c* reduction [13].

Since the primary biological function of cyt *c* is to carry out reduction–oxidation reaction, it follows that study of the interaction with nitroxide species is very important to its understanding. It is very difficult to study nitroxide species in living organism that is why the NO-mimetic models are useful for this purpose.

The potential component for biomimetic model of reduction–oxidation of NO species activity is the unique bis-nitroxide malonate methanofullerene molecule $C_{60}$, containing two NO-radical groups with the properties of the bis- and multi-site radical traps *in vivo* [14], and that it is able to immobilize the biologically active substances in the monolayer [15]. Moreover, the C60 fragment can be considered as the electron with drawing polyolefin capable of having oxidizing properties (Scheme 1).

Therefore, the bis-nitroxide malonate methanofullerene can take part in different kinds of oxidation–reduction processes. Biomimetic bis-nitroxide malonate methanofullerene redox system draws great interest both in basic studies of NO-related processes as well as for new medicine and biosensor development.

A Langmuir monolayer is a useful model due to its simplicity and versatility. In particular, the molecular density of a monolayer is easily controlled at the air–water interface with a Langmuir film balance. This type of experimental design can be used to elucidate the redox state changes of $(NO^{\bullet})_2$-MF monolayers too, because the limiting area $A_0$ of $(NO^{\bullet})_2$-MF depends on charge–charge interactions between monolayer and subphase components [15]. At neutral pH (pH 5–7) limiting area of $(NO^{\bullet})_2$-MF in the monolayer was close to theoretical value of *ca.* 0.86 $nm^2$ for hexagonally close-packed fullerene molecules and to the experimental value of limiting area of $(NO^{\bullet})_2$-MF monolayer [15]. In acid medium the aggregation of $(NO^{\bullet})_2$-MF and decreasing of $A_0$ were observed; but the limiting area was increased significantly (repulsive forces) at pH 10 or in the presence of electron donor in subphase solution [15].

Besides, the monolayers transferred onto solid support from water subphase allow to study the redox processes using ESR and UV–vis spectra when reductant or oxidant is present in the aqueous solution. So, the Langmuir monolayers and adlayers of aqueous-insoluble $(NO^{\bullet})_2$-MF on solid support as NO-mimetic may be used for study its interaction with water-soluble biological active compounds.

It is very important to estimate the role of nitroxide species in the redox processes with commercial nitroxide TEMPO being excellent model for this test. Unfortunately TEMPO can not form monolayers, but it can immobilizate on solid support by a sorption from non-aqueous solution.

In this paper we have studied bis-nitroxide malonate methanofullerene $(NO^{\bullet})_2$-MF, being component of the Langmuir monolayers or of the adsorbate on solid support (silica gel and quartz) as a biomimetic model of reduction–oxidation interaction between NO species and biological active compounds, which play a role an antioxidant in living organism.

These results were compared with the reaction of commercial nitroxide TEMPO and nitric oxide being generated by sodium nitrite in the presence of ascorbic acid with the cyt *c*. The typical antioxidants as well dihydroquercetin (DHQ), ascorbic acid (AA) and synthetic drug—1-(β-oxyethyl)-4,6-dimethyl-1,2-dihydro-2-oxopyrimidine (xymedon) as cytochrome *c* in oxidized form were used for this research.

The antioxidant ability of $(NO^{\bullet})_2$-MF was estimated using $Fe^{3+}/Fe^{2+}$ changes of cytochrome c heme by UV–vis and EPR-spectra. Moreover, influence of bis-nitroxide malonate methanofullerene to the antioxidant activity of the biological active compounds (DHQ, AA, xymedon) was determined in the experiments on rats.

## 2. Experimental

### 2.1. Materials and reagents

Bis-nitroxide malonate methanofullerene $(NO^{\bullet})_2$-MF was synthesized according to the procedures described in Ref. [13] and was identified by UV, IR, $^{13}C$ NMR, ESR methods and by single-crystal X-ray diffraction analysis. MALDI-TOF MS, found *m*/*z* 1131.21; calculated: 1131.18 [13].

Cytochrome *c* (from horse heart) (≥95%, lot STBB7839V, "Fluka" (USA) "Sigma–Aldrich"), solvents (analytical grade), sodium nitrite (>99.9%), 2,2,6,6-tetramethylpiperidine-1-oxyl radical (TEMPO) (>99.9%), ascorbic acid (>99.9%), dihydroquercetin (DHQ) (>99.9%), phosphoric, succinic acid were purchased from Sigma–Aldrich and used without further purification, xymedon® (1-(β-oxyethyl)-4,6-dimethyl-1,2-dihydro-2-oxopyrimidine) (>99.9%) were purchased from "Crystal" (Russia).

### 2.2. Nitric oxide preparation

NO solutions was prepared by the addition of 2 M $H_2SO_4$ to solid $NaNO_2$ in a Kipps apparatus. The NO gas passed through four NaOH (20%) traps (to remove $NO_2$), and then through a solid $CO_2$ trap. The gas was collected in a phosphate buffer solution that had undergone four vacuum/$N_2$ deoxygenation cycles. The NO concentration in the solution varied from 1.2 to 2 mM. The $NO_2$-concentration was approx. 300 μM.

### 2.3. Silica gel with sorbed nitroxide species

Silica gel with sorbed nitroxide species ($(NO^{\bullet})_2$-MF or TEMPO) were prepared using $SiO_2$ sorbent (60, 15–49, 40–63 and 63–200 μ, Merck) treated with chloroform solution of nitroxide compounds with following drying at room temperature under vacuum 100 mm within 1 h.

### 2.4. Langmuir films and monolayers

Experiments were provided using Nima LB Deposition Trough 112D (KSV Nima, Sweden) system applying deionized water (resistivity > 18 MΩ cm, Simplicity, Millipore Inc.) with pH 5.5 as a

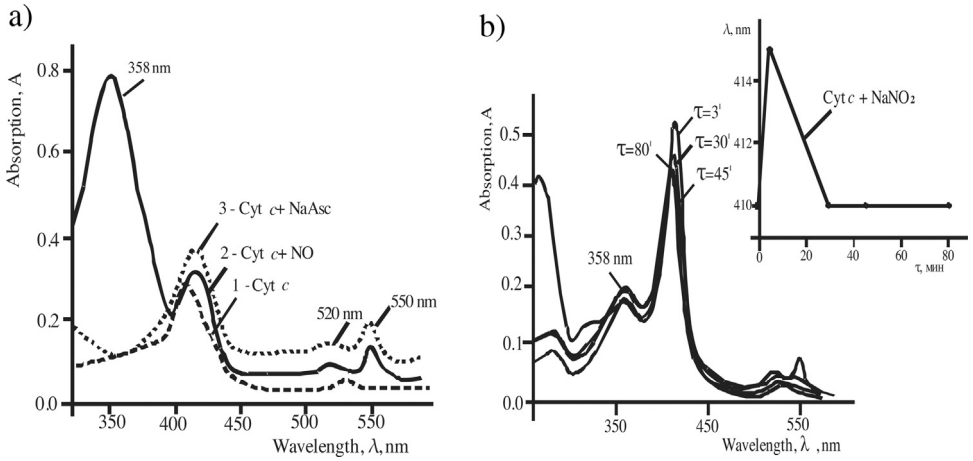


**Fig. 1.** UV–vis spectra of cyt *c* solution: (a) 2.4 μM cyt *c* – oxidized form – in water (*curve* 1, broken line), 2.4 × μM cyt *c* after addition nitric oxide (*curve* 2, solid line), 3.5 × μM cyt *c* – reduced form – after addition $5 \times 10^{-4}$ M sodium ascorbate (*curve* 3, dashed line), (b) the reaction mixture of $1 \times 10^{-5}$ M cyt *c*, $1.45 \times 10^{-2}$ M sodium nitrite, $5 \times 10^{-4}$ sodium ascorbate, $8.5 \times 10^{-3}$ M succinic acid in time. The insert shows dependence $\lambda = f(\tau)$.

subphase at 20 ± 1 °C. Wilhelmy plate method was used for registration of the surface pressure–area ($\pi$–$A$) isotherms at 20 ± 1 °C. The time of solvent evaporation and compression speed were chosen to provide as low hysteresis of the films as possible. Compression of the film was provided in continuous mode at the rate of 60 $cm^2$/min by two symmetric frames. Spreading solutions was prepared by dissolving the appropriate amount of compound $(NO^{\bullet})_2$-MF in chloroform (concentration 1.0 mg/mL). Then 20 μL of the solution was spread on the aqueous subphase with a chromatographic microsyringe in several stages; solvent evaporation and equilibration of the amphiphile on the interface took 30–40 min. $(NO^{\bullet})_2$-MF ($1 \times 10^{-8}$ mol) was spread on the subphase surface. Surface pressure $\pi = \gamma_0 - \gamma$, $\gamma_0$ and $\gamma$ [mN $m^{-1}$] that is surface tension before and after the spraying monolayers. Limiting area (area per molecule) $A_0$ of $(NO^{\bullet})_2$-MF was determinated in the intersection point of linear part the $\pi$–$A$ isotherm and horizontal axis. Surface compressional modulus $Cs^{-1}$ of 2D-films was calculated by the following equation:

$$Cs^{-1} = -A_0(d\pi/dA)_{P,T,ni}[mN/m]$$

where $A_0$—limiting area.

### 2.5. Absorption spectra

Absorption spectra of the aqueous solutions were recorded by "Bio line Specord S-100" (Analytik Jena), 10 mm quartz cuvette. Spectrophotometer error is 0.002 units transmittance at $4.5 \times 10^{-5}$ M cytochrome *c*, the relative standard deviation (RSD%) being 0.9%.

### 2.6. EPR

EPR spectra were obtained using Bruker EMX spectrometer at room temperature. $C_{60}(NO^{\bullet})_2$-MF thin film on $SiO_2$ solid support was placed with a special syring (2 mL) at room temperature. Dynamic changes of EPR signal were estimated having put the solid support into cyt *c* solution with time.

### 2.7. Biomedical research

Pharmacological effects on rats were studied in accordance with the requirements of the current Principles of Good Laboratory Practice (Russia, State Standard R 53434-2009). The experiment was carried out by using 30 Wistar male rats. Three groups of animals were parted, those were exposed to contact thermal burn under

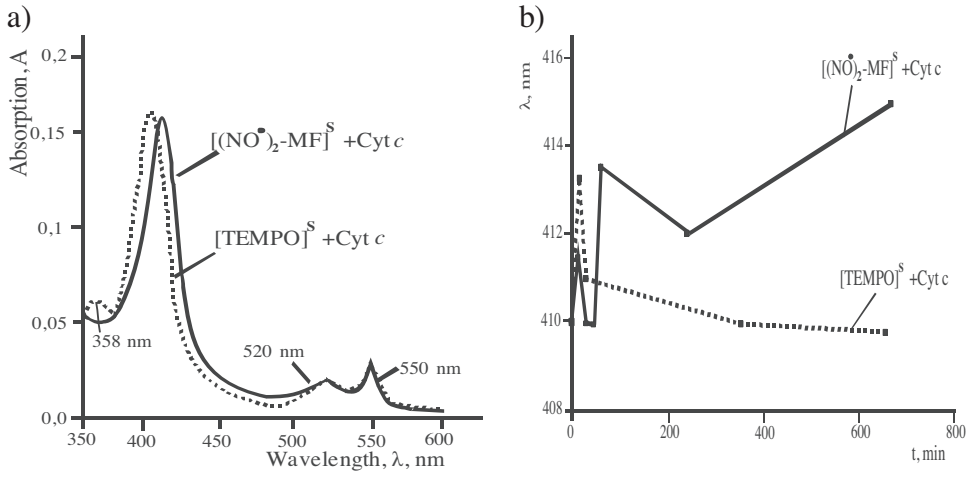


**Fig. 2.** UV–vis spectral data of cyt *c* solution after TEMPO treatment (broken line) or bis-nitroxide methanofullerene (solid line) sorbed on $SiO_2$. (a) $A = f(\lambda)$ after 10 h; (b) $\lambda = f(\tau)$, where $\tau$—time of cyt *c* interaction with the sorbent.

anesthesia (the burn area is 20% of the body surface). After thermal injury modeling a pharmaceutical composition was applied to the wound surface of the animals in the main group ($n = 10$) for 10 days. The animals in the first control group ($n = 10$) were treated with 10% xymedon-containing ointment (xymedon −10 g, levomicetin −0.75 g, polyethylenoxydes: PEO-1500 −19.05 g, PEO-400 −70.2 g), and in the second control group they were not treated. The pharmaceutical composition consisted of levomicetin −0.75 g, xymedon −10 g, polyethylenoxydes: PEO-1500 −19.05 g, PEO-400 −70.1 g, bis-nitroxide malonate methanofullerene $(NO^{\bullet})_2$-MF −0.1 g.

The catalase activity was estimated in the tissue extract by using Aebi method [16], based on the ability of hydrogen peroxide to give stable coloration with ammonium molybdate. The catalase activity was expressed in units of $min^{-1}\ g^{-1}{}_{tissue}$. SOD activity in tissue extracts was estimated by the Nischikimi method [17], based on the enzyme's ability to inhibit the restoration in the presence of nitro blue tetrazolium and phenazine methosulfate NADH.

The intensity of lipid peroxidation was estimated by spectrophotometry using conjugated diene and triene containing in the product after the extraction of lipids from the supernatant of chloroform–methanol solution [18].

Chemiluminescent analysis of lipid peroxidation (LP) intensivity induced by ferrous-ions and peroxide hydrogen in blood was estimated using the method [19].

Statistical analysis of the data was performed using Statistica 6.0 program [20], and Kolmogorov–Smirnov test. Statistical significance was evaluated by the comparison of qualitative effects in pairs of distributions using Fisher's test; Mann–Whitney criterion U test for independent samples was used to compare the groups using quantitative parameter.

## 3. Results and discussion

UV–vis spectra control of the interaction cyt *c* with $(NO^{\bullet})_2$-MF and TEMPO on silica gel support was performed compared to spectra of the reaction mixtures of cyt *c* and gaseous NO or $NaNO_2$. Earlier we had shown the changes of UV–vis spectrum of the aqueous solution of cyt *c* following the addition of gaseous NO during 15 min [21]. The shift of $\gamma$-band at 410 nm to 415 nm characterizing the reduced form cyt *c* was observed (Fig. 1a). Moreover, new intensive band at 358 nm, two weak bands—520 nm ($\beta$) and 550 nm ($\alpha$) typical for cyt $c^{2+}$ appeared. Sodium ascorbate was added for spectrum control of cyt *c* reduced form using the absorption of $\alpha$- (550 nm), $\beta$- (520 nm) and $\gamma$- (415 nm) bands. In this case, at pH 7.1 the initial oxidized form of cytochrome *c* (cyt $c^{3+}$) which has the band at $\lambda_{max}$ 410 nm converts into reduced form of cyt $c^{2+}$ completely (Fig. 1a).

Sodium nitrite in the aqueous solution of cyt *c* in the presence of biogenic acid (ascorbic, succinic, tartaric and citric) leads to NO formation and, as a result, to heme structure changes. UV–vis spectrum of the aqueous solution of reaction mixture during 15 min is similar to spectrum of the solution after gaseous NO addition in cyt *c* (Fig. 1a).

We believe UV–vis spectra indicate the changes of heme from cyt $c^{3+}$ to cyt $c^{2+}$, but also the formation of different nitrosyl cyt c complexes with nitric oxide ($\lambda_{max}$ 358 nm).

Earlier we had estimated the regeneration and the local microcirculation effects of the pharmaceutical composition (combined gel) containing cyt $c^{3+}$, sodium ascorbate and sodium nitrite [21]. At the initial stage the interaction cyt *c* with nitrite-ascorbate system in acid medium, probably, leads to two types of complexes—NO–cyt $c^{2+}$($\lambda_{max}$ 415 nm) and nitrosyl cyt $c^{2+}$–$NO^{+}$ ($\lambda_{max}$ 358 nm), yet NO–cyt $c^{2+}$-complex is not stable and converts to NO–cyt $c^{3+}$ complex ($\lambda_{max}$ 410 nm) with time (Fig. 1b). The positive effects in the wound healing is not only due to the action of NO or nitrosyl-

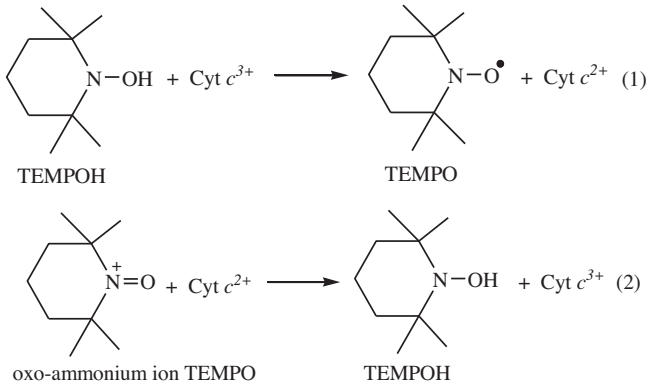


**Scheme 2.** The proposed mechanism of TEMPO interaction with cytochrome *c*.

containing cytochrome *c*-complexes, but also due to the excess of antioxidant – sodium ascorbate – in pharmaceutical composition, since metabolism of NO and related N-oxides in the systemic circulation that depends on concentration of blood antioxidants. When human plasma is exposed to NO or $NO_2$, a rapid loss in antioxidants, such as ascorbic acid, uric acid and most important protein thiols, occurs [22].

UV–vis spectra of cyt *c* solution after its interaction with TEMPO or $(NO^{\bullet})_2$-MF sorbed on $SiO_2$ changed with time (Fig. 2). During the first 30 min $\alpha$- (550 nm) and $\beta$- (520 nm) bands typical for cyt $c^{2+}$ appeared; but $\gamma$- (415 nm) band position differed in the systems [TEMPO-cyt *c*] and [$(NO^{\bullet})_2$-MF–cyt *c*]. The changes in the spectrum region of 410–550 nm after ten hours is demonstrated on Fig. 2a.

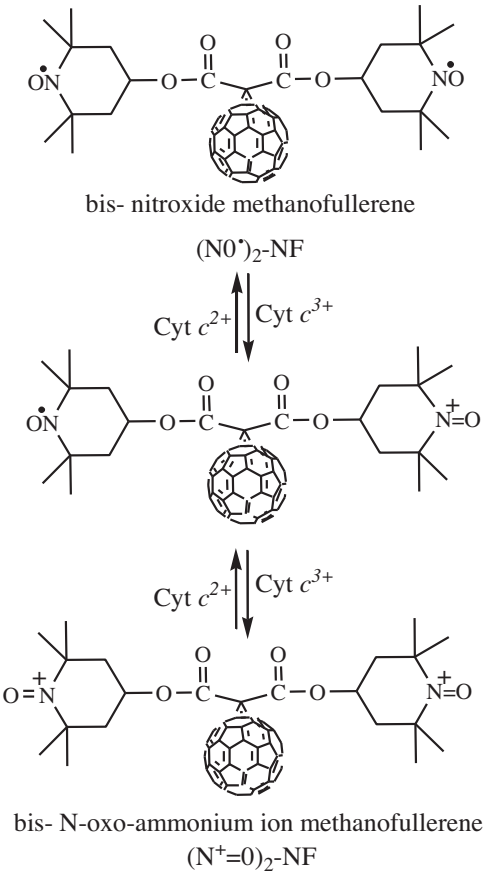


**Scheme 3.** The proposed redox reaction of bis-nitroxide methanofullerene $(NO^{\bullet})_2$-MF with cyt *c*.

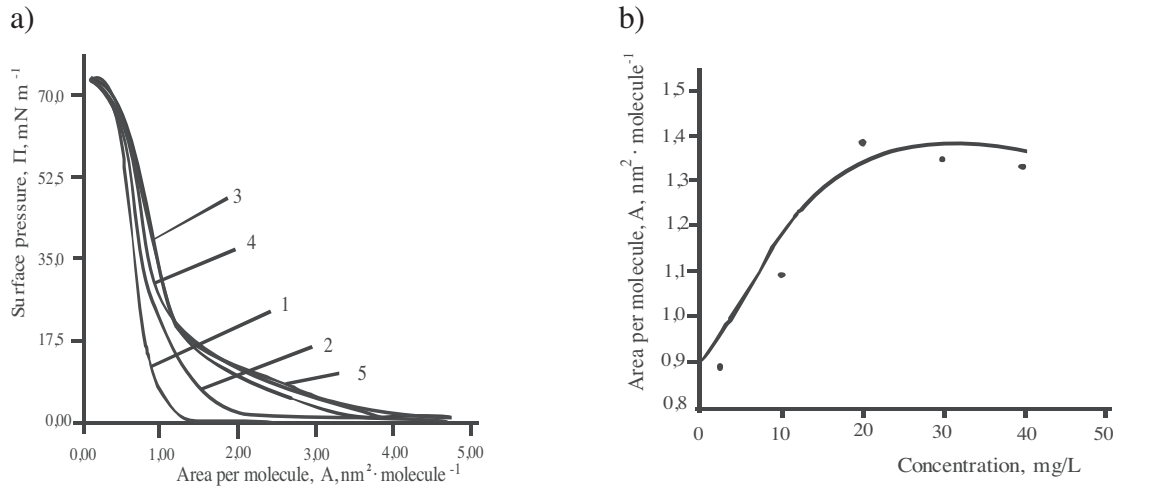


| №curves | Cyt *c* aqueous subphase, mg-L$^{-1}$ | $A_o$, nm$^2$ | Cs$^{-1}$, mN/m |
|---|---|---|---|
| 1 | - | 0.88±0.03 | 185±4 |
| - | 5 | 0.89±0.03 | 142±3 |
| 2 | 10 | 1.10±0.02 | 138±5 |
| 3 | 20 | 1.35±0.03 | 129±4 |
| 4 | 30 | 1.40±0.03 | 126±3 |
| 5 | 40 | 1.37±0.03 | 123±5 |

**Fig. 3.** The influence of cytochrome *c* on $(NO^{\bullet})_2$-MF monolayer state: (a) surface pressure *versus* area per molecule $\pi = f(A)$, cytochrome *c* concentration in the subphase (mg L$^{-1}$), (b) the dependence of limiting area $A_0$ on the concentration of cytochrome *c* in the subphase (SD = 4% mean ± SD, $n = 5$).

Fig. 2b shows the dynamic of $\gamma$-band changes: during ten hours $\gamma$-band of cyt *c* in the system containing TEMPO corresponded $\gamma$-band for cyt $c^{3+}$ (broken line), but in the system [$(NO^{\bullet})_2$–cyt *c*] $\gamma$-band characterized the reduced form cyt $c^{2+}$ (solid line).

Therefore, the reduction of iron(III) in heme cyt *c* in the presence of TEMPO was reversible, but the reduction of iron(III) was irreversible when $(NO^{\bullet})_2$-MF was used. Taking in attention, that the formal redox potential for the ferri/ferrocytochrome *c* couple in buffer solution at pH 7 is 0.265 V *versus* NHE, may be proposed the value of redox potential for $(NO^{\bullet})_2$-MF more than for cyt *c*. The proposed mechanism of TEMPO interaction with cyt *c* is presented in Scheme 2. During this process the oxo-ammonium ion $TEMPO^+$ is continuously regenerated *in situ* with a primary oxidant ($O_2$, $Fe^{3+}$cyt *c*).

Thus, visible spectra of Fe-heme in cyt c may be used as the indicator of the interaction of cyt *c* with nitroxide species *in vitro*, and $(NO^{\bullet})_2$-MF can be a reductant in relation to compounds in the case of their redox potential is less.

Fig. 3a shows $\pi$–*A* isotherms of $(NO^{\bullet})_2$-MF on pure water subphase (*curve* 1) and on cyt *c* containing aqueous subphase (*curves* 2–5) at 290 K. The limiting area $A_0$ of the films increases upon addition of cyt *c* in the subphase from 0.88 nm$^2$ for pure water

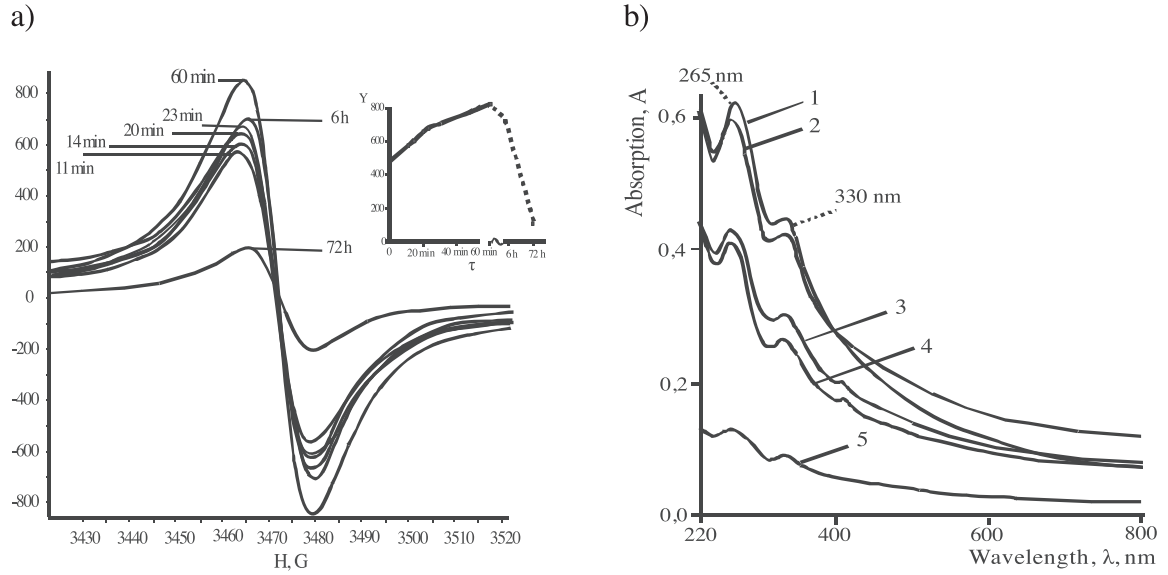


**Fig. 4.** The changes of spectra of thin films of $(NO^{\bullet})_2$-MF on quartz after immersion into cyt *c* solution in time: (a) ESR—spectra into $4 \times 10^{-5}$ M cyt *c* solution: 1–11 min, 2–14 min, 3–20 min, 4–23 min, 5–60 min, 6–6 h, 7–72 h, (b) UV–vis spectra into $1 \times 10^{-5}$ M cyt *c* solution: 1–10 min, 2–40 min, 3–60 min, 4–80 min, 5–90 min.

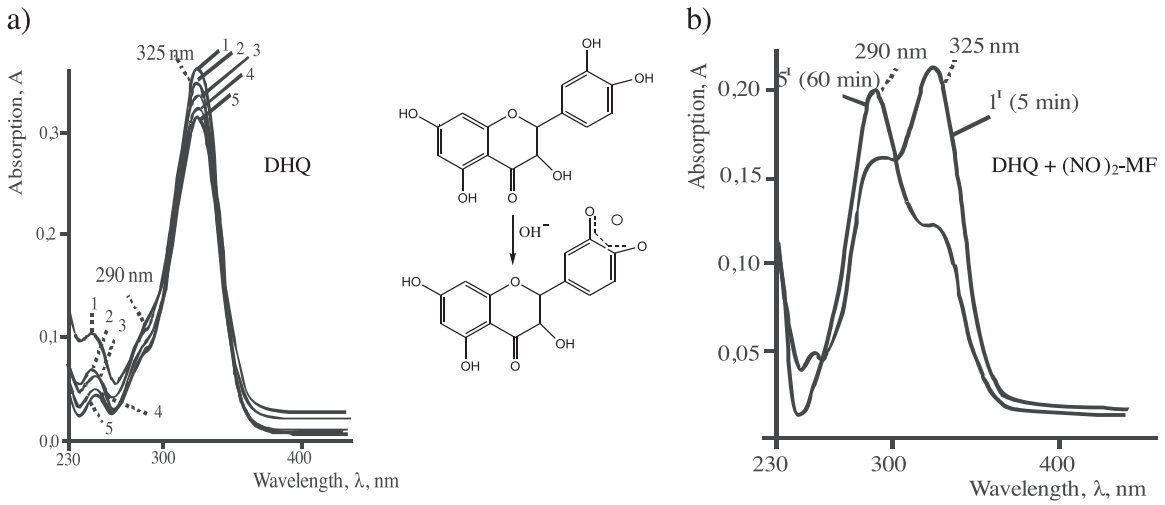


**Fig. 5.** UV–vis spectra: (a) of $2 \times 10^{-5}$ M DHQ in solution $4 \times 10^{-5}$ M NaOH in time: the aqueous solution of DHQ without $(NO^{\bullet})_2$-MF monolayers: 1–5 min, 2–10 min, 3–25 min, 4–40 min, 5–60 min, (b) the aqueous subphase under $(NO^{\bullet})_2$-MF monolayers: 1′–5 min; 2′–60 min.

to 1.40 $nm^2$ in the presence of cyt *c*. The dependence of the limiting area $(NO^{\bullet})_2$-MF monolayers on concentration of cyt *c* in the subphase was formal represented as Langmuir-type adsorption isotherm with plateau in the range $1.35 \pm 0.05$ $nm^2$, that exceeds $A_0$ for the homogenous monolayer $(NO^{\bullet})_2$-MF 1.5-fold.

Unlike the increase of limiting area the collapse pressure for $(NO^{\bullet})_2$-MF monolayers does not change in the presence of cyt *c* which reflects an invariability of the monolayers composition, excluding the immobilization of cyt *c* in monolayers. This behavior can be explained in terms of electrostatic repulsion between the positive oxo-ammonium ions headgroups of fullerene under action cyt *c* (Scheme 3).

This is associated with a decrease in surface compressional modulus $Cs^{-1}$ from 185 to 123 mN/m (Fig. 3). The compressional modulus $Cs^{-1}$ can be used to characterize the phase state of the monolayer and to tract the phase transitions during isothermal compression. The value of $Cs^{-1}$ ranges approximately between 1000 and 2000 mN/m for solid-condensed films, between 100 and 250 for liquid-condensed monolayers, and between 10 and 50 for liquid-expanded phases and is about $\pi$ for ideal surface films [23]. The decrease of surface compressional modulus $Cs^{-1}$ for $(NO^{\bullet})_2$-MF monolayers on cyt *c* containing subphase can be explained by formation a liquid-condensed phase with less than close packing of $(NO^{\bullet})_2$-MF molecules in the monolayers on water subphase.

These data (limiting area and compressional modulus changes) and the absence of hysterisis in the "compression–distension" cycle and the results reproducibility allow to consider properties of monolayers $(NO^{\bullet})_2$-MF on cyt *c* subphase as the biomimetic response of the interaction of cyt *c* and NO moiety of $(NO^{\bullet})_2$-MF.

The changes with time in ESR spectra of $(NO^{\bullet})_2$-MF monolayers transferred on quartz and then treated by cyt *c* solution confirm oxo-ammonium ion $(NO^{\bullet})_2$-MF formation (Fig. 4a). The signal intensity of NO in thin films $(NO^{\bullet})_2$-MF under action cyt *c* was revealed to be changed with time: at first it increased in 60 min, then it decreased slowly. At the same time the decreasing of optical density in the region of 265 nm and 330 nm of visible spectra significantly (Fig. 4b).

The increase of EPR signal may be explained by Scheme 3 where a monoradical species are formed on the first stage (causing the growth of EPR signal intensity) and then diamagnetic bis-*N*-oxo-ammonium ion of methanofullerene or the structures of TEMPOH type (Eqs. (1) and (2)) are formed and EPR signal decreases.

Therefore, as well UV–vis and ESR spectra data of $(NO^{\bullet})_2$-MF films on quartz or on adlayers as the increasing of limiting area of

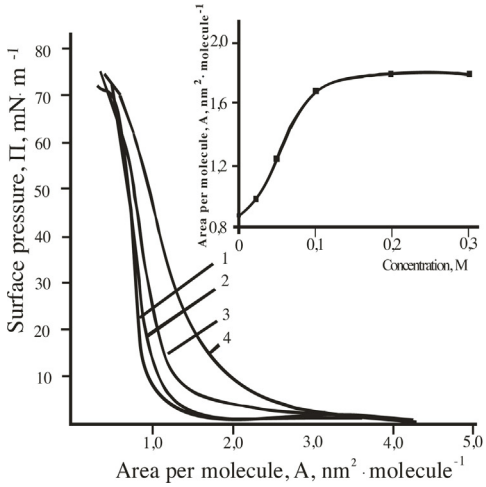


| $C_{xymedon}$, M | $A_0 \pm 0.02$, $nm^2 \cdot molecule^{-1}$ (n=5) | $Cs^{-1} \pm 0.04$, $mN \cdot m^{-1}$ (n=5) |
|---|---|---|
| - | 0.88 | 185 |
| 0.025 | 0.98 | 167 |
| 0.05 | 1.26 | 164 |
| 0.1 | 1.70 | 187 |
| 0.2 | 1.70 | 187 |
| 0.3 | 1.70 | 187 |

**Fig. 6.** The influence of xymedon concentration on $(NO^{\bullet})_2$-MF monolayers state. $\pi$–*A* isotherms of $(NO^{\bullet})_2$-MF monolayers on aqueous subphase of xymedon. The insert shows dependence of limiting area *A* on xymedon concentration *C*.

**Table 1**
The properties of $(NO^{\bullet})_2$-MF monolayers—limiting area $A_O$ and surface compressional modulus $Cs^{-1}$ ($SD$ = 4% mean ± SD, $n$ = 5).

| Subphasecomponent (pH) | $A_0$(nm2 molecule−1) | $Cs^{-1}$(mN m−1) | Schematic model of $(NO^{\bullet})_2$-MF films |
|---|---|---|---|
| (pH 5.6) | 0.88 ± 0.03 | 185 ± 3 | 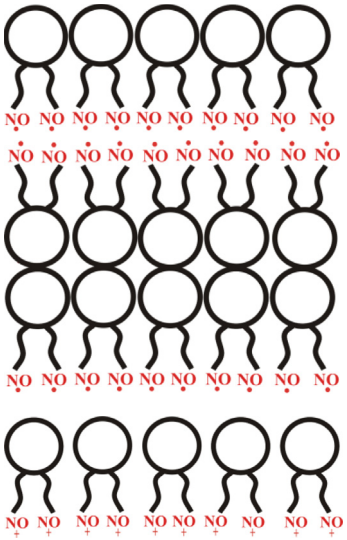 |
| cyt *c* (pH 5.6) | 1.10 ± 0.03 | 138 ± 4 | |
| (pH 3.6) | 0.42 ± 0.03 | 88 ± 5 | |
| cyt *c*(pH 3.6) | 0.42 ± 0.03 | 88 ± 5 | |
| cyt *c*, AA (pH 3.6) | 0.42 ± 0.03 | 88 ± 5 | |
| DHQ (pH 3.2) | 0.43 ± 0.02 | 88 ± 5 | |
| cyt *c*, NaAsc (pH 6.2) | 1.10 ± 0.03 | 138 ± 4 | |
| AA (pH 10.0) | 1.00 ± 0.02 | 70 ± 4 | |
| DHQ (pH 10.0) | 1.10 ± 0.02 | 110 ± 4 | |

$(NO^{\bullet})_2$-MF monolayers on the cyt *c* containing subphase, confirm the interaction of $(NO^{\bullet})_2$ radicals, mainly, with $Fe^{2+}$ in the porphyrin heme of cyt c and, eventually, the disappearance of nitroxide radical moiety.

The properties of the monolayers $(NO^{\bullet})_2$-MF on cyt *c* containing subphase in the presence of the reductants –ascorbic acid (AA) and sodium ascorbate depended on pH. The limiting area $A_0$ of $(NO^{\bullet})_2$-MF decreased from 0.88 $nm^2$ (water subphase) and 1.10 $nm^2$ (cyt *c* containing subphase) to 0.42 $nm^2$ for monolayers on cyt *c* containing subphase in the presence of AA at pH 3–4. At the same time the surface compressional modulus ($Cs^{-1}$) was decreased from 185 and 138 mN/m, consequently, to 88 mN/m (Table 1).

The similar changes of $(NO^{\bullet})_2$-MF monolayers on water, dihydroquercetin (DHQ) or cyt *c* containing aqueous subphase at pH 3 were observed. The two fold decrease of the limiting area can be related to the formation of bilayers. In fact, the limiting area value is about half the area predicted by the theoretical value for C60-fullerene moiety. Schematic model of $(NO^{\bullet})_2$-MF films is given in Table 1.

It can be assumed that these results are due to the association or the aggregation of $(NO^{\bullet})_2$-MF molecules in monolayer up to bilayer formation on the aqueous subphase which is specific for fullerene core in the acidic media [15,24]. At pH 10 or in neutral medium the limiting area $A_0$ of $(NO^{\bullet})_2$-MF was increased insignificantly. These data can be explained by the fullerene disaggregation that is similar to the process of disaggregation in the presence of electron donor in the polar media under the action of light inducing the formation of the intermediate superoxide anion-radical [24].

The spectra changes of the DHQ in the aqueous solution in the presence of $(NO^{\bullet})_2$-MF sorbed on silica gel was estimated (Fig. 5). At the initial stage DHQ was in oxidized form (quinoid form) at pH 10.0, taking into account that UV–spectrum of oxidized DHQ is characterized by the one band with $\lambda_{max}$ = 325 nm [25] (reduced form of DHQ has the band in the region $\lambda_{max}$ = 290 nm with shoulder $\lambda$ = 325 nm). It has been shown, that in the presence of $O_2$ and $(NO^{\bullet})_2$-MF–$SiO_2$, a fraction of oxidized DHQ was drastically decreased. In the case of DHQ the band with $\lambda_{max}$ = 290 nm which characterize reduced form of DHQ was appeared (Fig. 5b).

Thus, $(NO^{\bullet})_2$-MF was able to reduce oxidized form DHQ, in consequence of reduced form having high antioxidant activity was regenerated.

The antioxidant activity of bis-nitroxide methanofullerene and its mixture with DHQ was studied on the blood of rats by chemiluminescent analysis of lipid peroxidation (LP) intensiveness induced by ferrous-ions and peroxide hydrogen. Antioxidant capacity ($I/S \times 10^2$) of DHQ was increased in the presence of $(NO^{\bullet})_2$-MF from 5.40 to 8.11 and normalization rate of LP (-tg2α) was decreased from 0.17 to 0.14. The analysis of LP products in the first stage—diene conjugates (DC) and triene conjugates (TC) and Schiff's bases (SchB) [17] showed 2-fold decreasing of these parameters (DC from 0.21 to 0.16, TC from 0.04 to 0.02, SchB from 4.24 to 2.17). So, we can see that $(NO^{\bullet})_2$-MF is able to increase antioxidant activity

**Table 2**
The effectiveness of burn treatment with ointment and xymedon in experiments on rats.

| The observed phenomenon | | Xymedon (10%) Control 1 | $(NO^{\bullet})_2$-MF (0.001%) + xymedon (10%) | Control 2 untreated |
|---|---|---|---|---|
| Granulation, days | | 3 | 3 | 4 |
| Wound cleansing, days | | 5 | 4 | 7 |
| Colonization, CFU $mL^{-1}$ | | $2.8 \times 10^8$ | $2.0 \times 10^8$ | $7.4 \times 10^8$ |
| Increase wound area, % | 3 days | 81 | 80 | 89 |
| | 7 days | 62 | 55 | 68 |
| | 11 days | 25 | 20 | 45 |
| Complete healing, days | | 14 | 12 | 19 |
| Antioxidant activity of catalase (15 days), mmol $min^{-1}$ $\mu g^{-1}$ of protein | | 2.7 | 3.8 | 1.4 |
| Antioxidant activity of superoxide dismutase (15 days), mmol $min^{-1}$ $\mu g^{-1}$ of protein | | 1700 | 2200 | 400 |

DHQ containing drugs, although they are capable to act as both an antioxidant and an oxidant.

These results can be used for studying the antioxidant activity of synthetic drugs not demonstrating reductant properties *in vitro* by contrast to DHQ having the redox potentials of $DHQ_{red}/DHQ_{ox}$ couple $E^0 = 0.55$ V.

These results was compared with water-soluble synthetic drug—1-(β-oxyethyl)-4,6-dimethyl-1,2-dihydro-2-oxopyrimidine (xymedon). It is known as effective immunomodulators, regenerant and reparant [26] due to its antioxidant activity *in vivo*, which use for treatment burn wounds.

It was interesting to study the mimetic interaction of xymedon with $(NO^{\bullet})_2$-MF using the monolayers model and the experiment burn treatment of dosage form xymedon by rats. The interaction of $(NO^{\bullet})_2$-MF monolayers with xymedon on the aqueous subphase is shown in Fig. 6.

It has been shown, that the dependence of the limiting molecular area $A_0$ of $(NO^{\bullet})_2$-MF on xymedon concentration C (Fig. 6) is similar to the dependence of $A_0 = f(C)$ on cyt *c* concentration in the subphase (Fig. 3b). The plateau on the isotherm $A_0 = f(C)$ was in the range $1.70 \pm 0.02$ nm$^2$. Two-fold increase of the limiting area $A_0$ of $(NO^{\bullet})_2$-MF characterizes very intensive interaction between $(NO^{\bullet})_2$-MF molecule and xymedon being electron donor.

We can assume that the properties of $(NO^{\bullet})_2$-MF monolayers on subphase containing biological active compounds—electron donors, depend on fullerene core state, too. The paradoxical properties of fullerene moiety C60 that can be a real effective radical scavenger but, at the same time, it is known to induce radical production upon photoirradiation. The light radiation excites C60 from the ground state to $C^1$60, a short-lived species readily converted to the long-lived $C^3$60. The latter can transfer energy to molecular oxygen, if present, going back to the ground state. In this way toxic $O_2{}^1$ is generated. Moreover, fullerene in singlet and triplet states can be easily reduced to C60—by electron transfer. All the reactive species herein described can attach biomolecules, and fullerenes can be considered as very effective 'radical sponges' [27,28] being capable of taking part in reversible redox processes.

The antioxidant properties were tested in the experiments on rats for burn wound treatment with 10% xymedon ointment (Table 2).

These experiments proved the ability of $(NO^{\bullet})_2$-MF to increase the antioxidant activity of xymedon. Such properties make bis-nitroxide malonate methanofullerene fullerene very interesting with respect to potential applications in the field of biomedical or pharmaceutical chemistry. Due to their inherent structural properties and their ability to act as radical sponges, fullerenes and their derivatives have been proposed as potent antioxidants.

## 4. Conclusion

Bis-nitroxide malonate methanofullerene$(NO^{\bullet})_2$-MF containing two NO-radical groups and π-conjugated fullerene moiety being fairly electronegative with ability to undergo multiple reversible reduction steps has been studied in the mimetic interaction of NO species with natural compounds which play a role of an antioxidant in living organism.

It has been shown, that Langmuir monolayers of $(NO^{\bullet})_2$-MF both on aqueous subphase and monolayers transferred onto solid support also adlayers on silica gel are a good tools for the estimation of the response of the mimetic interaction of NO species with antioxidants. The changes of the properties such as the limiting area value, surface compressional modulus, the paramagnetism, UV–vis characteristics of the thin films in the presence of ferrocytochrome *c* or oxidized form of dihydroquercetin may indicate to the oxo-ammonium ion formation in the system.

The advantages of this biomimetic approach are high reproducibility of results, the properties dependence of $(NO^{\bullet})_2$-MF monolayers on composition aqueous subphase as the biomimetic response of the interaction of biological active compounds of subphase and NO moiety, and the stability of NO containing phase in contrast to exogenic NO species.

The reaction of ferrocytochrome *c* with NO radical groups of the fullerene may be used as a standard model of the oxidation and reduction processes involving NO species, because it is similar to its interaction with gaseous nitric oxide. It can be proposed that the value of redox potential for $(NO^{\bullet})_2$-MF more than for the ferri/ferrocytochrome *c* couple.

Bis-nitroxide malonate methanofullerene showed excellent scavenging activity against a reactive oxygen species as well an individual compound as the combination with antioxidants such as dihydroquercetin and xymedon® in the experiments on rats.

The mimetic behavior of the oxidation–reduction processes and antioxidant activity make bis-nitroxide malonate methanofullerene very interesting with respect to potential application in biosensors and new medicines development.

## Appendix A. Supplementary data

Supplementary data associated with this article can be found, in the online version, at http://dx.doi.org/10.1016/j.colsurfb.2015.09.026.

## References


[1] A.N. Osipov, G.G. Borisenco, Y.A. Vladimirov, Biological role of nitrosyl complexes of heme, Success Biol. Chem. 47 (2007) 259–292.
[2] K.N. Hall, J. Garthwaite, What is the real physiological NO concentration in vivo? Nitric Oxide 21 (2009) 92–103.
[3] C. Opländer, A. Römer, A. Paunel-Görgülü, et al., Dermal application of nitric oxide *in vivo*: kinetics, biological responses, and therapeutic potential in humans, Clin. Pharmacol. Ther. 91 (6) (2012) 1074–1082.
[4] J.O. Lundberg, E. Weitzberg, M.T. Gladwin, The Nitrate–Nitrite–Nitric Oxide Pathway in Physiology and Therapeutics, Nature Publishing Group, 2008, http://dx.doi.org/10.1038/nrd2466.
[5] F.X. Guix, I. Uribesalgo, M. Coma, F.J. Muñoz, The physiology and pathophysiology of nitric oxide in the brain, Prog. Neurobiol. 76 (2) (2005) 126–152.
[6] T. Yoshitomi, Y. Nagasaki, Nitroxyl radical-containing nanoparticles for novel nanomedicine against oxidative stress injury, Nanomedicine 6 (3) (2011) 509–518.
[7] Jian-An Jiang, Jia-Lei Du, Zhan-Guo Wang, Zhan-Nan Zhang, Xi Xu, Gan-Lin Zheng, Ya-Fei Ji, Practical $Cu(OAc)_2$/TEMPO-catalyzed selective aerobic alcohol oxidation under ambient conditions in aqueous acetonitrile, Tetrahedron Lett. 55 (2014) 1677–1681.
[8] A. Samuni, S. Goldstein, A. Russo, J.B. Mitchell, M.C. Krishna, P. Neta, Kinetics and mechanism of hydroxyl radical and OH-adduct radical reactions with nitroxides and with their hydroxylamines, J. Am. Chem. Soc. 124 (2002) 8719–8724.
[9] M.C. Krishna, A. Russo, J.B. Mitchell, S. Goldstein, H. Dafni, A. Samuni, Do nitroxides antioxidants act as scavenges of superoxide or as SOD mimics? J. Biol. Chem. 271 (1996) 26026–26031.
[10] S.E. Solovieva, R.A. Safiullin, E.N. Kochetkov, N.B. Melnikova, M.K. Kadirov, E.V. Popova, I.S. Antipin, A.I. Konovalov, Langmuir monolayers and thin films of amphifilic thiacalix[4]arenes. Properties and matrix for the immobilization of cytochrome *c*, Langmuir 30 (15) (2014) 15153–15161.
[11] J.R. Stone, R.H. Sands, W.R. Dunham, M.A. Marletta, Electron paramagnetic resonance spectral evidence for the formation of a pentacoordinate nitrosyl-heme complex on soluble guanylatecyclase, Biochem. Biophys. Res. Commun. 207 (1995) 572.
[12] A.N. Osipov, G.O. Stepanov, Y.A. Vladimirov, A.V. Kozlov, V.E. Kagan, Regulation of cytochrome *c* peroxidase activity by nitric oxide and laser irradiation, Biochemistry 71 (10) (2006) 222.
[13] M.C. Krishna, A. Samuni, J. Taira, S. Goldstein, J.B. Mitchell, A. Russo, Stimulation of nitroxides of catalase-like activity of hemoproteins, J. Biol. Chem. 271 (1996) 26018–26025.
[14] V.P. Gubskaya, L.Sh. Berezhnaya, A.T. Gubaidullin, I.I. Faingold, R.A. Kotelnikova, N.P. Konovalova, V.I. Morozov, I.A. Litvinov, L.A. Nuretdinov, Synthesis, structure and biological activity of nitroxide malonate methanofullerens, Org. Biomol. Chem. 5 (2007) 976–981.
[15] N.B. Melnikova, I.V. Gulyaev, M.V. Gulenova, A.A. Volkov, O.E. Zimnyakova, V.P. Gubskaya, L.Sh. Berezhnaya, A.T. Gubaidullin, Structure of surface films of

malonate mono- and dinitroxyl methanofullerenes, Russ. Chem. Bull. Ser. Chem. 9 (2008) 1920–1931.
[16] H. Aebi, Catalase, in: H.V. Bergmeyer (Ed.), Methods in Enzymatic Analysis, Academic Press, New York, 1974, pp. 673–684.
[17] M. Nishikimi, N.A. Rao, K. Yagi, The occurrence of superoxide anion in the reaction of reduced phenasine methasulphate and molecular oxygen, Biochem. Biophys. Res. Commun. 46 (2) (1972) 849–857.
[18] V.Z. Lankin, Enzymatic oxidation of lipids, Ukr. Biochem. J. 56 (3) (1984) 317–331.
[19] Y.H. Siddique, G. Ara, M. Afzal, A. Muslim, Estimation of lipid peroxidation induced by hydrogen peroxide in cultured human lymphocytes, Dose Response 10 (2012).
[20] O.U. Rebrova, Statistical analysis of medical data. Application of package of STATISTICA applied programs, M.: Media Sfera (2006) 312.
[21] V.M. Korobko, N.B. Melnikova, D.A. Panteleev, A.K. Martusevich, S.P. Peretyagin, The study of the complexes of nitromedicine with cytochrome *c* and NO-containing aqueous dosage form in the wound treatment of rats, Nitric Oxide 42 (2014) 62–69.
[22] B. Halliwell, M.-L. Hu, S. Louie, T.R. Duvall, B.K. Tarkington, P. Motchnik, C.E. Cross, Interaction of nitrogen dioxide with human plasma, FEBS Lett. 313 (1992) 62–66.
[23] Y.T. Davies, E.K. Rideal, Interfacial Phenomena, Academic Press, New York, 1961 (Chapter 3).
[24] L.B. Piotrovsky, O.I. Kiselev, Fullerenes in Biology, Publishing Office, Rostok, St. Petersburg, 2006.
[25] N.B. Melnikova, E.N. Kochetkov, S.E. Solov'eva, E.V. Popova, I.S. Antipin, A.E. Bol'shakova, O.E. Zhiltsova, A.I. Konovalov, tert-Butylthiacalix[4]arene monolayers as a biomimetic model for the oxidation of antioxidants with cytochrome *c*, Russ. Chem. Bull. 9 (2011) 1948–1955.
[26] S.G. Ismaylov, G.A. Ismaylov, M.Yu. Averynov, V.S. Resnik, Xymedon in Clinical Practice, NGMA, N. Novgorod, 2001.
[27] P.J. Krusic, E. Wasserman, P.N. Keizer, J.R. Morton, K.F. Preston, Radical reactions of C60, Science 254 (1991) 1183–1185.
[28] C.N. McEwen, R.G. McKay, B.S. Larsen, C60 as a radical sponge, J. Am. Chem. Soc. 114 (1992) 4412–4414.